https://doi.org/10.5194/egusphere-2026-4111
Preprint. Discussion started: 21 July 2026

Cross-scale characteristics of extreme precipitation events under climate change

Jingkun Yang[1], Benjamin Poschlod[2,3], Felix Ament[3]

[1] Faculty of Mathematics, Informatics and Natural Sciences, Universität Hamburg, 20146 Hamburg, Germany
[2] Institute for Global Water Security, Hamburg University of Technology, 21079 Hamburg, Germany
[3] Earth and Society Research Hub (ESRAH), Universität Hamburg, 20146 Hamburg, Germany

Correspondence to: benjamin.poschlod@tuhh.de

Abstract

Extreme precipitation is intensifying globally, with Central Europe emerging as a hotspot for accelerating hydroclimatic risks. Traditional hazard metrics often fail to capture the spatial extent and compound temporal characteristics of these events. This study employs the cross-scale Weather Extremity Index (xWEI) – a metric integrating intensity, duration, and area – to systematically analyze the 200 most extreme precipitation events over Germany. Using high-resolution (3 km) convection-permitting COSMO-CLM simulations under the RCP8.5 scenario, we compare event characteristics across historical (1971–2000), present (1990–2019), and future (2031–2060; 2071–2100) climate states. Our results reveal a profound intensification: averaged over the top 200 events and relative to the historical baseline, the xWEI is projected to increase by 27 % and 45 % until the near and far futures, respectively. This is driven by increasing peak rainfall intensity, accompanied by a fundamental structural shift in the extreme-event population of the top 200 events. The composition transitions from being dominated by short-lived (1–4 h), small-scale (< 5,000 km²) events toward more persistent (12–24 h) and spatially extensive rainfall systems. Furthermore, we demonstrate that the perceived severity of these changes depends on the statistical frame of reference. When return periods are re-calibrated ("adapted") to each specific climate period, adjusting for the dominant effect of peak intensification, they reveal a second-order intensification that remains hidden in traditional assessments. This effect, diagnosed primarily between the historical and subsequent climates, manifests as a rise in the cross-duration and cross-space characteristics: events are becoming more extreme across a broader range of durations and areas simultaneously, significantly expanding the total volume of extreme precipitation. These findings highlight the emergence of more complex, high-impact hazard structures that necessitate the multi-scale assessment capabilities of the xWEI framework.

1 Introduction

Extreme precipitation on different time scales is the trigger of manifold hazards, such as urban flooding, flash floods, river floods, landslides, posing severe risks to the society, infrastructure, and agriculture. Observations and model simulations consistently indicate increases in both the frequency and intensity of precipitation extremes under global warming, broadly consistent with the Clausius–Clapeyron scaling (Gimeno et al., 2022). Climate models further suggest continued intensification throughout the 21st century, particularly across mid- and high-latitudes and humid tropical regions (Gimeno et al., 2022; Madsen et al., 2014; Prein et al., 2017; Poschlod and Ludwig, 2021; Kotz et al., 2023). Under high-emission scenarios (RCP8.5), approximately 46 % of global land areas may face moderate-to-high risks from changing precipitation extremes (Huang et al., 2021). Even small increases in rainfall intensity can trigger disproportionate and nonlinear impacts (Munz et al., 2024), exposing limitations of conventional metrics based on point intensity or fixed return periods. Such metrics fail to capture the spatial extent and compound characteristics of evolving hazards (Pöschmann et al., 2021). As sub-daily extremes intensify (Barbero et al., 2017; Westra et al., 2014), multiscale assessment becomes essential.

Europe is emerging as a hotspot for accelerating hydroclimatic risk. Observations reveal intensification of both short- and long-duration extremes in Central Europe (Zeder and Fischer, 2020; Haslinger et al., 2025). Regional projections indicate that short-duration event intensity and spatial extent may increase by up to 300 % under RCP8.5 by the end of the century (Nissen and Ulbrich, 2017), while rare sub-daily extremes could become up to three times more frequent (Hosseinzadehtalaei et al., 2020). Germany has experienced several severe flood events, including the 2002 Elbe flood (€10 billion losses), the 2013 Danube–Elbe floods (€8 billion losses), and the July 2021 flood in western Germany (€33 billion in total losses). While these riverine events were triggered by large-scale atmospheric drivers, also local urban flooding and flash floods are reported, which are driven by localized convective downpours (Caldas-Alvarez et al., 2022; Thieken et al., 2022; Piper et al., 2016), illustrating that impacts arise from diverse processes across spatial and temporal scales. The June 2013 floods, for instance, were large-scale from the outset, affecting the Danube and Elbe catchments and resulting in extensive riverine flooding (Khazai et al., 2013; Thieken et al., 2016). By contrast, the 29 June 2017 event in Berlin was highly localized, caused by an intense convective downpour that led to urban inundation without evolving into a broader catchment-scale flood (Caldas-Alvarez et al., 2022). Such complexity underscores the need for indices integrating intensity, duration, and spatial extent.

In response to the limitations of conventional extreme precipitation metrics, Müller and Kaspar (2014) introduced the Weather Extremity Index (WEI), which combines rarity (mean logarithmic return period) and spatial footprint (weighted area) to quantify event extremeness and identify the scale of maximum impact relevance. However, by focusing on peak extremeness at a single scale, WEI overlooks the temporal compound structure of events. Voit and Heistermann (2022) therefore proposed the cross-scale Weather Extremity Index (xWEI), integrating extremeness across all relevant durations and areas. Defined as a double integral over the logarithms of duration and area, xWEI captures total extremeness volume across scales and reveals compound structures not identifiable through point-based measures. To estimate the extremeness, the duration-dependent Generalized Extreme Value (dGEV; Koutsoyiannis et al., 1998) distribution is applied in the xWEI framework, which is fit consistently across durations capturing the temporal characteristics of extreme precipitation (Fauer et al., 2021; Rischmuller et al., 2026; Ulrich et al., 2020).

Although xWEI has been demonstrated using high-resolution radar observations for Germany (2001–2021, Voit and Heistermann, 2022), its application to climate projections remains unexplored. Consequently, the influence of climate change on the cross-scale structure of extreme precipitation events is still unclear. In turn, Rybka et al. (2023) conclude that an event-based statistical assessment of convection-permitting climate simulations would be a valuable addition. In this study, we newly

https://doi.org/10.5194/egusphere-2026-4111
Preprint. Discussion started: 21 July 2026

apply the xWEI on convection-permitting climate projections over Germany under the high-emission scenario RCP8.5. Thereby, we tackle a key methodological challenge concerning the parameterization of the extreme value statistical assessment under a non-stationary climate. On the one hand, we estimate the rareness of events based on a dGEV fit to the historical climate ("fixed dGEV"). On the other hand, we re-fit the dGEV to future time periods ("adapted dGEV"). We note that these two strategies imply fundamentally different interpretations of extremeness affecting the projected cross-scale characteristics diagnosed by the xWEI. Going beyond pointwise assessments of intensity and frequency per rainfall duration, we aim to investigate climate change effects on the cross-scale characteristics of extreme precipitation events including intensities and areas across multiple durations.

2 Data

We use regional climate model simulations performed with COSMO-CLM v5.0-16 (Haller et al., 2022) to analyse extreme precipitation over central Europe, including Germany and its neighboring regions (Fig. 1). COSMO-CLM is run at a convection-permitting horizontal grid spacing of ~3 km, with consistent physical parameterizations and model configuration across all simulations. Lateral boundary conditions are provided by global reanalysis or climate model data at the domain edges.

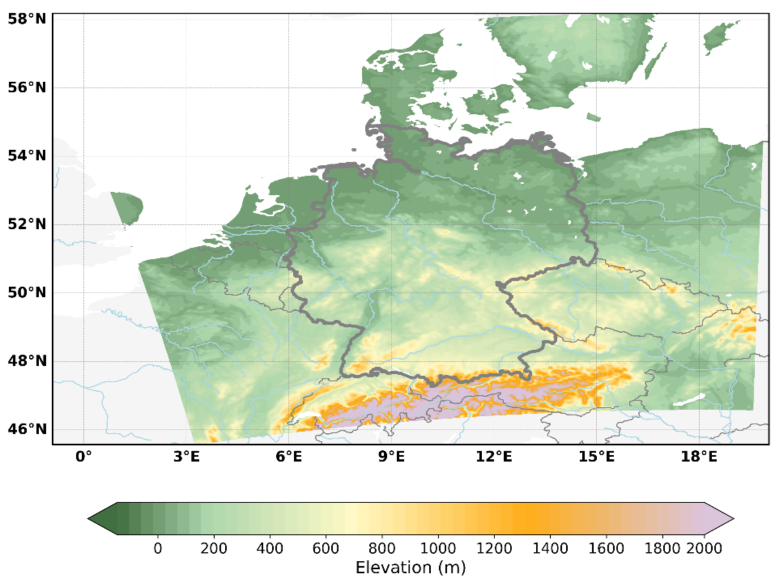

Figure 1: Spatial extent and elevation of the COSMO-CLM simulation domain over Central Europe. The thick gray line indicates the border of Germany.

To assess changes in extreme precipitation under past and future climate conditions, we consider four simulations covering different time slices. The first is a reanalysis-driven evaluation simulation, HoKliSim-De (Brienen et al., 2022), which dynamically downscales ERA5 (1979–2019) and ERA-40 (1971–1978), serving as an observationally constrained reference.

https://doi.org/10.5194/egusphere-2026-4111
Preprint. Discussion started: 21 July 2026

For the current climate, we use the period 1990–2019. The remaining three simulations are 30-year climate model experiments using the same COSMO-CLM setup but forced by boundary conditions from MIROC5 (CMIP5 configuration; Watanabe et al., 2011). These include (i) a historical baseline simulation (1971–2000; Haller et al., 2022a), (ii) a near-future projection (2031–2060; Haller et al., 2022b), and (iii) a far-future projection (2071–2100; Haller et al., 2022b), with the future projections driven under the high-emission scenario RCP8.5 (Riahi et al., 2011).
The CLM simulations of the future climate might inherit biases and characteristics from the driving global MIROC5 model. On a global scale MIROC5 shows an equilibrium climate sensitivity of 2.7 K, which places it at the lower end of the CMIP5 model range (2.1–4.7 K; Forster et al., 2013; Andrews et al., 2012). Evaluations of its historical performance have identified a slight cold bias in global mean surface temperature, which has been attributed to an overestimation of low-cloud cover leading to excessive shortwave reflection (Watanabe et al., 2011; Sakamoto et al., 2012). Furthermore, MIROC5 is among the driest models in the CMIP5 ensemble, with a mean global precipitation rate significantly lower than both the multi-model mean and observations (Flato et al., 2013; Sperber et al., 2013). Regarding its performance over Europe, MIROC5 is generally regarded as a median-performing model. It captures the large-scale atmospheric circulation reasonably well but exhibits typical model biases, most notably a warm and dry summer bias over the Mediterranean region (Vautard et al., 2021). Despite these shortcomings, MIROC5 has been widely used as a driving model for regional downscaling in EURO-CORDEX and related projects, including COSMO-CLM applications. At the regional scale, the dynamical downscaling adds spatial resolution and more detailed process representation, which help to reduce coarse-scale biases (Sørland et al., 2021). The COSMO-CLM simulations applied in this study have been evaluated for extreme precipitation on a grid cell level by Rybka et al. (2023) showing only a slight wet bias and good reproduction of the spatial pattern compared to observations. Lennartz et al. (2026) assess the intensity and frequency of hourly extreme precipitation per grid cell over Germany based on these climate projections. Consequently, the COSMO-CLM simulations provide a consistent framework for investigating climate-change signals in precipitation extremes under the RCP8.5 scenario.

3 Methods

To investigate extreme precipitation events and their changes under different climate conditions, the methodology applied in this study consists of two main steps. First, spatiotemporally coherent precipitation events are identified from hourly precipitation fields based on fixed thresholds by the German Weather Service (DWD). Second, the xWEI is derived for each detected event by incorporating its return period and computing the WEI, which together quantify the event's severity.

3.1 Definition and Identification of heavy precipitation events

3.1.1 Rainfall objects

https://doi.org/10.5194/egusphere-2026-4111
Preprint. Discussion started: 21 July 2026

A rainfall object is defined as a spatially contiguous region of precipitation that exceeds a duration-specific intensity threshold at a given time step, following the object-based heavy precipitation detection approach of Lengfeld et al. (2021), as adapted by Voit and Heistermann (2022) and based on the DWD severe weather warning thresholds (Table 1). Thresholds for non-standard durations (e.g. 2 or 4 hours) are linearly interpolated between adjacent official durations.

Table 1. Thresholds for heavy precipitation for event detection based on DWDs Warning Level 3 for severe weather

Duration (h)	1	2	4	6	12	24	48	72
Precipitation (mm)	25	27	31	35	40	50	60	90

Rainfall objects are identified using a multi-stage detection algorithm accounting for intensity and spatial coherence. For each hourly time series of precipitation files (Fig. 2a), rolling precipitation sums are computed for predefined accumulation durations t. Each sum is calculated over t consecutive hourly time steps and compared with the corresponding duration-specific threshold (Table 1). At each time step, a binary exceedance mask is generated, where grid cells meeting or exceeding the threshold are assigned a value of one (Fig. 2b). Spatially contiguous regions are identified using 8-connected component labeling (3×3 kernel), allowing diagonal adjacency. Candidate regions are validated by their spatial extent, computed as the number of grid cells multiplied by 9 km². A duration-dependent minimum area criterion is applied: 9 km² for $t \leq 3$ h and $t \times 3$ km² for $t > 3$ h. Regions not meeting these criteria are excluded (Fig. 2c).

3.1.2 Calculation of return periods

The identification of rainfall events and the xWEI calculation depend on reliable estimates of return periods for multiple durations. Therefore, we adapt the duration-dependent Generalized Extreme Value (dGEV) distribution, established by Koutsoyiannis et al. (1998) and advanced by Ulrich et al. (2020), and applied by Voit and Heistermann (2022). The dGEV models extreme precipitation intensity directly within a GEV framework, incorporating duration dependence into its parameters. As shown in Equation 1 (Ulrich et al., 2020), *G(z,t)* represents the cumulative distribution function of annual maximum rainfall accumulations, describing the probability that the accumulation over a duration *t* does not exceed a threshold *z*. Duration dependence is incorporated into the GEV distribution through scaling relationships for the location ($\tilde{\mu}$) and scale (σ_0) parameters, characterized by a duration offset (θ) and a duration exponent (η), while the shape parameter (ξ) is assumed constant across durations. This approach estimates duration-parameterized functions jointly across all timescales, pooling data from different durations to stabilize return levels and maintain physical consistency. For each grid cell, dGEV parameters are estimated using the R package IDF (Ulrich et al., 2020).

$$G(z,t;\tilde{\mu},\sigma_0,\xi,\theta,\eta) = exp\{-[1+\xi(\frac{z}{\sigma_0(t+\theta)^{-\eta}}-\tilde{\mu})]^{-1/\xi}\} \qquad (1)$$

The return period at each grid cell is estimated from the observed precipitation intensity (*z*) using the dGEV distribution, as shown in Equation 2.

https://doi.org/10.5194/egusphere-2026-4111
Preprint. Discussion started: 21 July 2026

$$p_{t,i} = \frac{1}{1-G(z,t)} \quad (2)$$

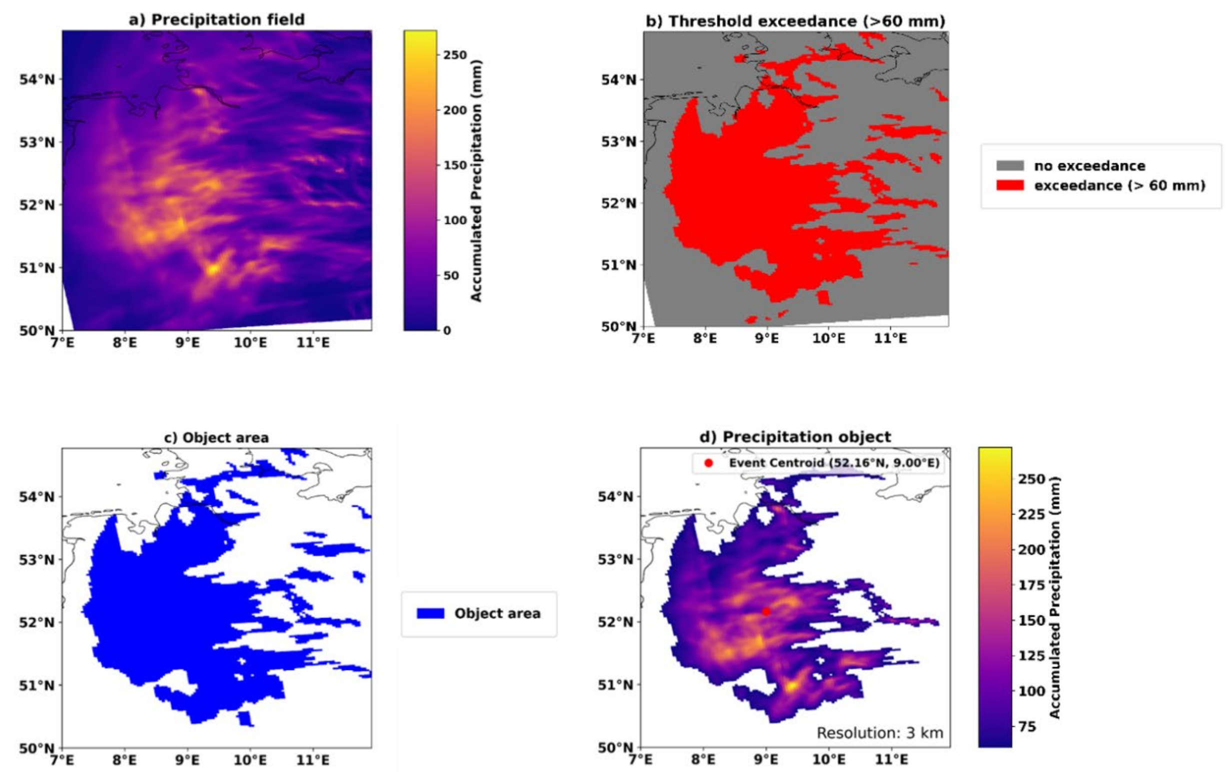

Figure 2. Scheme for identification of heavy precipitation objects (48 h event Jul2002): Precipitation accumulation field at a given time step (a), threshold exceedance mask for heavy precipitation (b), heavy precipitation areas satisfying the minimum size criterion (c), and identified heavy precipitation object (d).

In this study, we apply two conceptually distinct approaches to address non-stationarity under climate change. In the fixed dGEV approach, dGEV parameters for the simulations driven by MIROC5 are estimated from the historical period (1971–2000), and future occurrence probabilities are evaluated using this fixed parameter set. This serves as the default setup, where the xWEI reflects changes in all event characteristics including the dominant effect of increasing rainfall intensity driven by a warmer climate (Martel et al., 2021; Purr et al., 2022). Conversely, in the adapted dGEV approach, dGEV parameters are re-estimated for the future periods (2031–2060 and 2071–2100). This allows the framework to explicitly account for evolving rainfall characteristics within the xWEI framework and thereby isolate how other event properties – such as spatial extent or cross-duration intensity – respond to changing climatic conditions. For the COSMO-CLM simulation driven by ERA5, we fit dGEV parameters separately. Even though the regional precipitation is modelled by COSMO-CLM in all four simulations, we argue that the boundary conditions of ERA5 and MIROC5 differ substantially. ERA5 as reanalysis products assimilates pressure, temperature, and humidity conditions, while MIROC5 runs freely. Furthermore, the atmospheric core of both model systems is fundamentally different (Kuma et al., 2023), which might lead to systematic deviations in the precipitation climates.

https://doi.org/10.5194/egusphere-2026-4111
Preprint. Discussion started: 21 July 2026

Hence, we refrain from applying dGEV parameters from COSMO-CLM driven by MIROC5 (1971–2000) on the simulation driven by ERA5.

3.1.3 Rainfall events

Rainfall events are derived from the rainfall objects through a two-stage filtering procedure (Fig.2) ensuring spatiotemporal independence and geographic location. For each object, the event severity is quantified using the E_{tA} metric, which integrates the spatial distribution of return periods within the event footprint. For an event with area A and valid return period values $p_{t,i}$ across n grid cells, E_{tA} is computed as:

$$E_{tA} = \frac{\sum_{i=1}^{n} ln(p_{t,i})}{n} \cdot \frac{\sqrt{A}}{\sqrt{\pi}} \quad (3)$$

where A is expressed in km^2. The arithmetic square root of A divided by π represents a weighted measure of the area (Müller and Kaspar, 2014).

A spatiotemporal filtering step is then applied to ensure event independence. Events are first sorted chronologically, and spatial overlap is determined by comparing the set of grid cells comprising each event. Following Lengfeld et al. (2021), we temporally decluster events requiring a gap g of at least 4 hours for $t \leq 4$ hours and $g \geq t$ for $t > 4$ hours. For overlapping events in space or time, the event with the higher E_{tA} value is retained. Finally, events are kept only if their centroid lies within Germany (Fig. 2d). The resulting catalogue comprises spatially and temporally independent rainfall events with quantified extremeness. This event extraction framework is applicable to a wide range of precipitation phenomena, from short-lived, small-scale convective bursts to long-lasting, large-scale rainfall systems.

3.2 Calculation of the cross-scale weather extremity index xWEI

The cross-scale weather extremity index (xWEI) by Voit and Heistermann (2022) extends the Weather Extremity Index (WEI) proposed by Müller and Kaspar (2014). The WEI quantifies the extremeness of a precipitation event at the single spatial–temporal scale where it reaches its maximum. The xWEI integrates across spatial and temporal scales, providing a measure of severity that reflects the compound nature of extreme precipitation events.

The computation of xWEI begins with the estimation of return periods for each grid cell and accumulation duration. Let $p_{t,i}$ denote the return period for grid cell i and duration t. Annual maxima are extracted for each cell and duration, and the dGEV is fitted to ensure consistency across durations. For a given duration t, all grid cells within the analysis domain are ranked in descending order of $p_{t,i}$, The extremeness at area (E_{tA}) for the top n ranked cells, which cover the total area of an event is computed, as described in Sect. 3.2.1. This process yields an E_{tA} curve for each duration, illustrating how extremeness varies with spatial extent (Fig. 3a). The WEI corresponds to the maximum value among all these curves, whereas the xWEI retains the entire set of E_{tA} values. E_{tA} curves for different durations are combined into a continuous surface $E_{tA}(A,t)$, defined in the

https://doi.org/10.5194/egusphere-2026-4111
Preprint. Discussion started: 21 July 2026

space of spatial extent A and the natural logarithm of duration ln(t) (Fig. 3b). The cross-scale extremeness is then quantified as the volume under this surface, thereby capturing the event severity across multiple spatial and temporal scales (Equation 4).

$$xWEI = \int_{ln(t)} \int_{A} E_{tA} dA d(ln(t)) \quad (4)$$

In line with Voit and Heistermann (2022), xWEI is computed within a fixed 200 × 200 km^2 square domain centred on the centroid of each event. This domain balances the representation of large-scale systems relevant to fluvial flooding and smaller-scale convective features important for pluvial and flash floods.

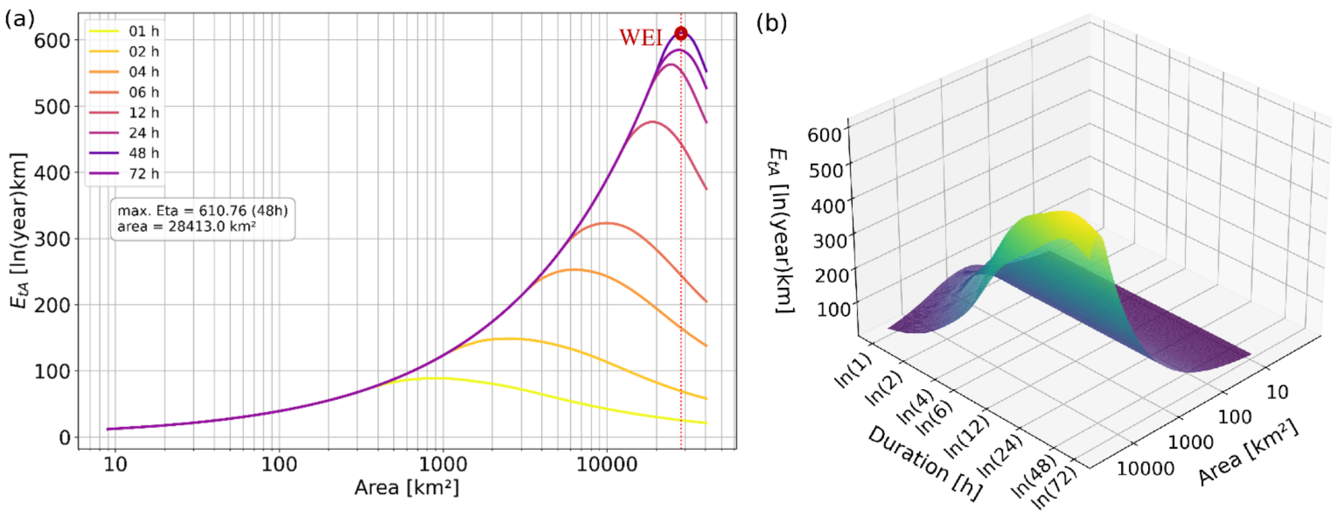

Figure 3. (a) E_{tA} curves for different durations plotted along the spatial dimension, with the WEI marked by a red circle. (b) E_{tA} values from (a) interpolated on a regular grid of logarithmic values of durations and area. The volume below the surface is a graphical representation of the xWEI capturing event extremity across space and durations. All plots display the same extreme precipitation event as in Figure 2.

4 Results

4.1 The 200 most extreme precipitation events under climate change

The 200 most extreme precipitation events over Germany are identified and ranked using the xWEI index for four periods: the ERA5-based present period (1990–2019), three climate model simulation periods representing the historical (1971–2000), near-future (2031–2060), and far-future (2071–2100) conditions. While the ERA5-based period serves as a reanalysis-observationally constrained reference, the three simulation datasets are evaluated within a fixed dGEV framework in which the parameters are derived solely from 1971–2000 and then consistently applied to the two future time periods.

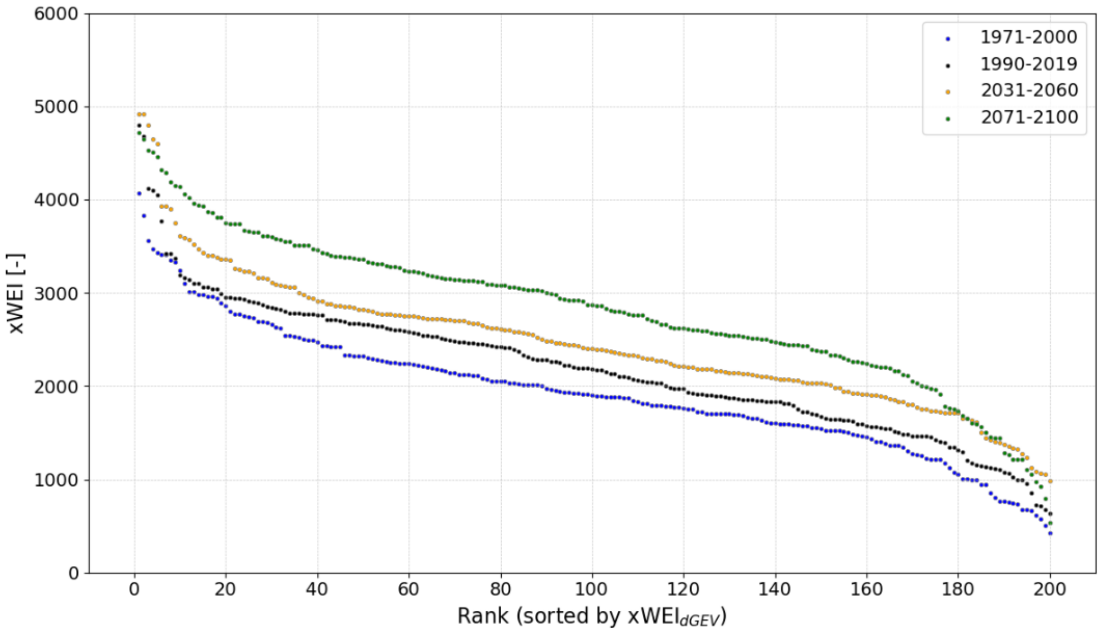

Figure 4. Ranked xWEI values of the 200 most extreme precipitation events, calculated using the fixed dGEV fitting procedure, across temporal horizons: past (1971–2000, blue), near-future (2031–2060, orange), and far-future (2071–2100, green). Note that for the present period (1990–2019) driven by ERA5, a separate dGEV is fitted to calculate the xWEI.

As shown in Figure 4, the xWEI values of the 200 most extreme events exhibit a systematic upward shift with time across the four simulations. On average, xWEI values increase by 27 % for the near future (2031–2060) and 45 % for the far future (2071–2100), respectively, compared to the past period (1971–2000). These results demonstrate a clear progression towards more extreme precipitation events under warming conditions. A quantile-based comparison further highlights the systematic nature of this shift. At the numbers for a selection of ranks: 25, 50, 100, 150, xWEI values in the far-future simulation are elevated by approximately 34 %, 45 %, 51 % and 54 %, respectively, relative to the past.

Since xWEI integrates intensity, spatial footprint and duration, it captures multiple facets of event severity. The top 200 xWEI-ranked events are therefore classified by spatial extent and grouped into duration classes (Figure 5). In the historical period (1971–2000), the sample is dominated by small-area events (< 5,000 km²), with considerable contributions from short and medium duration events. By contrast, the future periods (2031–2060 and 2071–2100) show a shift toward larger spatial scales (5,000–10,000 km²), and medium and long duration events account for an increasing share of the top-ranked extremes; this tendency is most pronounced in the far future. It is important to note that each period is analyzed independently, with exactly 200 events selected according to the highest xWEI values. As the underlying extreme-event population evolves under climate change, the composition of the top-ranked subset shifts toward larger and more persistent events, while smaller, short-lived extremes become less represented. These changes should therefore be interpreted as a shift in the relative prominence of different event types among the most extreme tails, rather than a direct change in absolute occurrence frequencies.

https://doi.org/10.5194/egusphere-2026-4111
Preprint. Discussion started: 21 July 2026

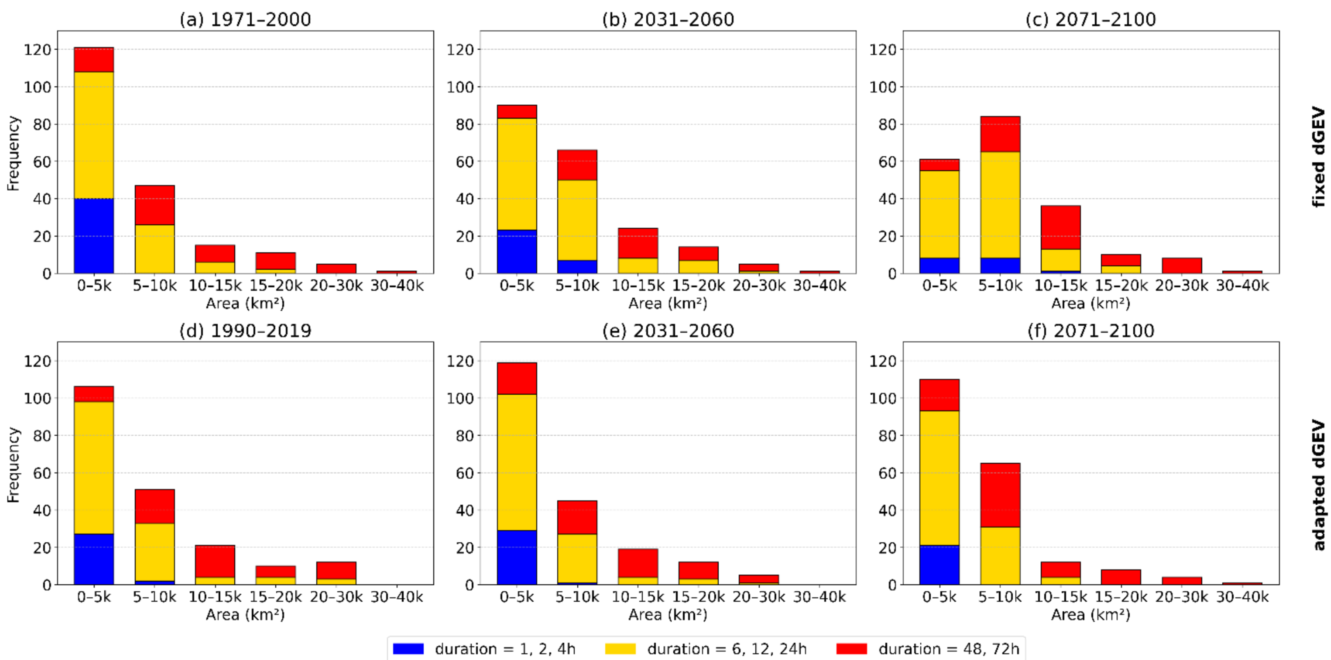

Figure 5. Stacked histograms of event areas at peak WEI for the top 200 events. (a) 1971–2000, (b) 2031–2060, and (c) 2071–2100 are based on the fixed dGEV fitting procedure. (d) 1990–2019, (e) 2031–2060, (f) 2071–2100 are based on the adapted dGEV fitting procedure. The indicated durations mark the temporal scale of the duration with the maximum WEI value.

4.2 Effects of choice of re-fitting the dGEV to future precipitation extremes

Since the fixed-dGEV approach serves as the main framework of this study, the adapted-dGEV experiment is explicitly treated as a comparative diagnostic. In the adapted-dGEV procedure, the dGEV parameters are re-estimated for each period, thereby adjusting the return periods to the period-specific climatology and adapting the perception of extreme intensities to a changed climate. As the adapted dGEV fits account for the shift in rainfall intensities under climate change, the effect of spatial characteristics and cross-duration characteristics are isolated.

The ranked xWEI values of the 200 most extreme events for the four simulations based on the adapted dGEV are shown in Figure 6. Compared with the fixed dGEV case, the differences between periods are considerably smaller. The upward shift of xWEI values that is evident under climate change (Figure 4) largely disappears, and the distributions of the future periods are now much closer to those of the past. This indicates that adapting the dGEV to each climate state tends to dampen the climate change signal in xWEI. Nevertheless, a clear shift relative to 1971–2000 remains: the mean xWEI increases by about 13 %, 15 %, and 15 % for the three subsequent periods, respectively. The most pronounced change occurs only once (Figure 6), namely between the past (1971–2000) and the subsequent periods (1990–2019 and beyond), while differences among the later periods remain comparatively small.

https://doi.org/10.5194/egusphere-2026-4111
Preprint. Discussion started: 21 July 2026

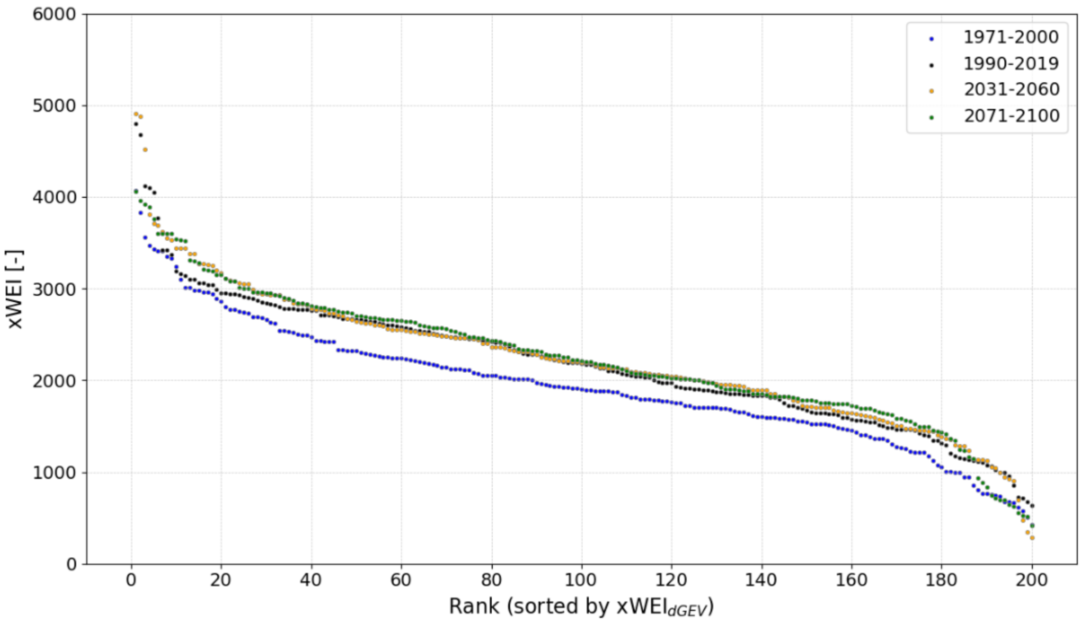

Figure 6. Ranked xWEI values of the 200 most extreme precipitation events, calculated using the adapted dGEV fitting procedure, across temporal horizons: past (1971–2000, blue), present (1990–2019, black), near-future (2031–2060, orange), and far-future (2071–2100, green).

The area distributions of the selected events provide additional support for this conclusion (Figure 5e and 5f). Across all four periods, the majority of events cluster within the smallest size class (< 5,000 km²), followed by progressively fewer events at larger spatial scales. Importantly, the frequency distributions of event areas remain nearly identical across periods, irrespective of whether events are dominated by short (1–4 h), intermediate (12–24 h), or long (48–72 h) accumulation durations. This consistent pattern can be attributed to the adapted dGEV fitting procedure, where the re-calibration of return periods across the durations results in a similar selection of events from the four periods across different durations and spatial scales.

4.3 Diagnosing the single shift in xWEI using intensity-based Eta integrals

A clear upward shift is observed only from the historical period (1971–2000) to the present climate (1990–2019) in the adapted dGEV framework (Fig. 6). Interestingly, Figure 5e and Figure 5f show only small increases in precipitation area for the peak WEI that can hardly explain this change in xWEI. Further, the intensity cannot cause the shift, as the adapted dGEV compensates for changes in precipitation intensity. To understand the origin of this behavior, we examined the spatial E_{tA} integral (Fig. 7), which is calculated within the fixed spatial domain (0–40000 km²) as proposed by Voit and Heistermann (2022). Although somewhat arbitrary, the range of spatial domain provides a compromise between capturing large-scale flood-related precipitation and retaining localized intense rainfall features, while ensuring comparability among events. Therefore,

https://doi.org/10.5194/egusphere-2026-4111
Preprint. Discussion started: 21 July 2026

variations in the E_{tA}-integral classes do not reflect changes in event size, but rather changes in rainfall intensity. For each of the top 200 extreme events per period, the E_{tA} integral is computed at eight different durations.

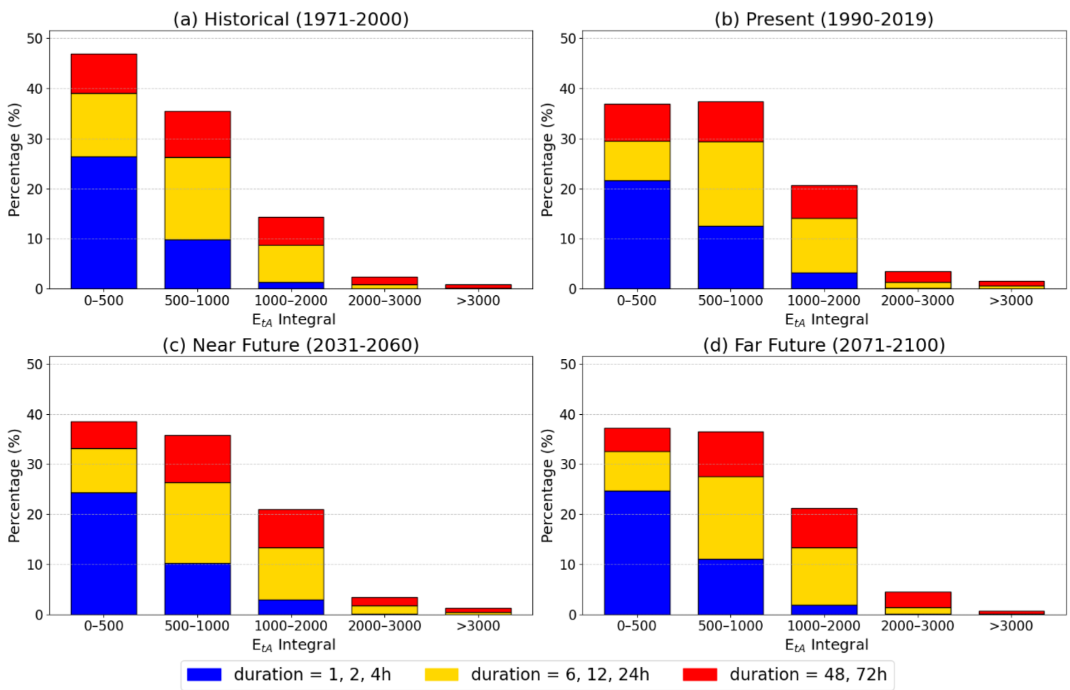

Figure 7. Percentage distribution of E_{tA} integral over area for the top 200 extreme events based on the adapted dGEV fitting procedure in four periods (1971–2000, 1990–2019, 2031–2060, 2071–2100).

While Figure 5 assesses the area and duration of the top 200 events at its duration with the maximum WEI, the E_{tA} integral approach considers all durations of the top 200 events and their integrated intensity across space. While the areas of the maximum WEI durations do not change notably with the adapted dGEV approach (Fig. 5), we find that the integral over E_{tA} (Fig. 7) increases from the historic to the present period. For the top 200 events, the short (1 h, 2 h, 4 h) and medium (6 h, 12 h, 24 h) durations exhibit a notable increase shifting from the 0–500 to the 500–1000 and 1000–2000 classes. The two future periods show a similar re-distribution of E_{tA} integrals as the present period. While the areas of the maximum WEI shows no notable changes, the cross-temporal extremity and area are diagnosed to rise. Using the graphical representation of Fig. 3a, one can imagine that the peak of the E_{tA} curves (i.e. the WEI) stays at similar values, while the shoulders of the curves rise leading to higher E_{tA} integrals. This behavior is consistent with the adapted dGEV framework, in which the intensity scaling is adjusted to each climate state and therefore limits a strong increase in peak intensities. Consequently, the increase in xWEI arises primarily from a broadening of elevated E_{tA} values across durations and areas rather than from higher peaks alone. Hence, the volume under the three-dimensional surface representing the xWEI (Fig. 3b) increases. While the fixed dGEV

https://doi.org/10.5194/egusphere-2026-4111
Preprint. Discussion started: 21 July 2026

approach jointly includes this second-order effect and rising peak intensities, the increase of xWEI values is dominated by the change in peak intensity (compare Fig. 4 and Fig. 6). In turn, (Fig. 4), the adapted dGEV excludes the effects of peak intensification (Fig. 6): E_{tA} is calculated based on the return periods $p_{t,i}$ (Eq. 3), where the adapted dGEV removes climate change effects on $p_{t,i}$ at each grid cell. Though, the E_{tA} integral metric detects intensification across space for short and medium durations, which we interpret as a second order effect of climate change on extreme precipitation events.

5 Discussion and Conclusions

Existing studies consistently indicate a general intensification of extreme precipitation under climate change, aligned with, below or above Clausius–Clapeyron scaling (~7 % per K; Berg and Haerter, 2013; Da Silva and Haerter, 2025; Lenderink et al., 2017; Lenderink et al., 2021; Schroeer and Kirchengast, 2018). Berg et al. (2019) assessed the multi-model EURO-CORDEX ensemble at 0.11° resolution and found that the scaling shows a high sensitivity to climate models, where the spatial scale of roughly 12km and parametrization of convection leads to an underestimation of hourly intensities. Convection-permitting models are found to improve intensities of sub-daily and daily rainfall extremes, the representation of the daily cycle, and the effect of complex topography on the spatial patterns of extreme precipitation (Dallan et al., 2023; Poschlod and Koh, 2024; Lucas-Picher et al., 2021; Berthou et al., 2020). Rybka et al. (2023) confirmed that COSMO-CLM at convection-permitting scale projects stronger precipitation intensities for future scenarios, particularly on sub-daily timescales.

Changes in event duration and spatial extent have also been highlighted. Hosseinzadehtalaei et al. (2020) reported that short-duration precipitation events (≤ 3 h) tend to intensify more strongly under warming, leading to steeper intensity–duration–frequency relationships. In contrast, our analysis, which focuses specifically on the 200 most extreme events, shows that the selection of short-lived extremes declines markedly, while medium- and long-duration events gain prominence. This difference likely arises from the event selection criteria and the estimation of extremity: by considering only the most extreme events, our study captures changes in high-impact events. In addition, the extremeness metric used in our analysis accounts not only for event duration but also for the spatial extent of each event. As a result, short-lived yet spatially confined precipitation events contribute less frequently to the top 200 most extreme events.

Poschlod et al. (2021) provided a European perspective, estimating 10-year return levels for sub-daily extremes. They highlight the important influence of internal climate variability on the estimation of rare quantiles and their scaling under climate change. This underlines the need for sufficiently large and robust event samples when assessing changes in extreme precipitation. Here, we pool the top 200 events across the German domain to derive a robust sample size for investigation and employ the dGEV, which is found to deliver more stable fits on small sample sizes than a conventional GEV (Rischmuller et al., 2026). Purr et al. (2021) demonstrated that in convection-permitting simulations for Germany, convective rain cells become more intense and larger under RCP8.5, with the strongest increases observed for the upper percentiles of intensity and cell area. Matte et al. (2022) reported an increase in the spatial extent of extreme precipitation events under warming, suggesting larger affected areas even when localized intensities remain constant or grow moderately.

https://doi.org/10.5194/egusphere-2026-4111
Preprint. Discussion started: 21 July 2026

From a cross-scale perspective, two consistent structural shifts emerge. First, in terms of event duration, the prevalence of short-lived extremes within the top 200 xWEI events become less represented, while medium- and long-duration events gain prominence, reflecting enhanced persistence of rainfall under warmer conditions. Second, with respect to spatial extent, small-scale extremes that dominate the historical record are increasingly replaced by medium-sized events, accompanied by a rising number of large-scale events in the future.

Finally, the analysis highlights the methodological sensitivity associated with the choice of dGEV parameterization. Under the fixed-dGEV framework, which anchors return periods to a historical baseline, climate change signals appear strongly, with future extremes becoming progressively more severe relative to the past. In contrast, the adapted-dGEV approach re-calibrates the parameters for each period, resulting in much smaller inter-period differences as the return-period mapping adapts to the evolving climatology. Diagnostics based on the E_{tA} integral over area help to explain this behavior. While the areas associated with the maximum-WEI durations show little change under the adapted-dGEV framework, the E_{tA} integral reveals a redistribution toward higher intensity classes from the historical to the present climate, particularly for short and medium durations, indicating an increase in the integrated spatiotemporal intensity of extreme events. Conceptually, this can be interpreted as a rise in the shoulders of the E_{tA} curves while their peaks remain similar. This implies that not only the most critical spatio-temporal scales intensify, but also neighbouring scales become more hazardous, increasing the likelihood of impactful events across a wider range of durations and affected areas. As a result, the E_{tA} integrals increase, leading to a greater volume under the three-dimensional xWEI surface. However, this redistribution occurs mainly between the historical and present climates, with little further systematic shift in future periods. Consequently, the adapted-dGEV results represent a "future perspective," where extremeness is evaluated relative to the contemporaneous climate, whereas the fixed-dGEV approach reflects a "past perspective," in which future events appear increasingly extreme relative to a stationary historical baseline. The xWEI framework can be applied for the evaluation of weather generators (Guan et al., 2025) or climate models against observations. Beyond that, we argue that the analysis of cross-scale characteristics via xWEI reveals novel insights into climate change effects on extreme precipitation events extending grid-cell based evaluation of rare quantiles. While our results are valid for only a single climate model, we recommend the application of the xWEI in both its "fixed dGEV" and "adapted dGEV" configurations to other convection-permitting climate simulations.

Code and data availability

Code and data for the extreme precipitation event identification and xWEI calculation are available from the following repository: https://doi.org/10.5281/zenodo.19877857 (Yang, 2026). The precipitation datasets used in this study are publicly available via the German Meteorological Service data portal. These include the reanalysis-driven HoKliSim-De simulation Brienen et al., 2022 (DOI: 10.5676/DWD/HOKLISIM_V2022.01) and the convection-permitting CPS simulations based on the MIROC5 model, including historical and future projections Haller et al., 2022a, b (DOIs: 10.5676/DWD/CPS_HIST_V2022.01; 10.5676/DWD/CPS_SCEN_V2022.01).

Author contributions

JY performed the data processing and analysis, including extreme event identification, xWEI calculation, and figure preparation. JY wrote the manuscript with contributions from BP and FA. BP and FA conceptualized the study and contributed to the methodology and manuscript revision.

Competing interests

The contact author has declared that neither of the authors has any competing interests.

Disclaimer

Copernicus Publications remains neutral with regard to jurisdictional claims made in the text, published maps, institutional affiliations, or any other geographical representation in this paper. While Copernicus Publications makes every effort to include appropriate place names, the final responsibility lies with the authors. Views expressed in the text are those of the authors and do not necessarily reflect the views of the publisher.

Acknowledgements

We would like to thank Paul Voit and Maik Heistermann for providing the publicly available code for calculating the xWEI index and Katharina Lengfeld and co-authors for the open access to their method regarding the extraction of extreme precipitation events. The authors used ChatGPT (GPT-4) by OpenAI and DeepSeek-R1 by DeepSeek to assist with the code development and to improve the readability of the text.

References

Andrews, T., Gregory, J. M., Webb, M. J., and Taylor, K. E.: Forcing, feedbacks and climate sensitivity in CMIP5 coupled atmosphere–ocean climate models, Geophys. Res. Lett., 39, https://doi.org/10.1029/2012GL051607, 2012.

Barbero, R., Fowler, H. J., Lenderink, G., and Blenkinsop, S.: Is the intensification of precipitation extremes with global warming better detected at hourly than daily resolutions?, Geophys. Res. Lett., 44, 974–983, https://doi.org/10.1002/2016GL071917, 2017.

Berg, P., Christensen, O. B., Klehmet, K., Lenderink, G., Olsson, J., Teichmann, C., and Yang, W..: Summertime precipitation extremes in a EURO-CORDEX 0.11° ensemble at an hourly resolution, Nat. Hazards Earth Syst. Sci., 19, 957–971, https://doi.org/10.5194/nhess-19-957-2019, 2019.

https://doi.org/10.5194/egusphere-2026-4111
Preprint. Discussion started: 21 July 2026

Berg, P. and Haerter, J. O.: Unexpected increase in precipitation intensity with temperature — A result of mixing of precipitation types? Atmos. Res., 119, 56–64, https://doi.org/10.1016/j.atmosres.2011.05.012, 2013.

Berthou, S., Kendon, E.J., Chan, S.C. Ban, N., Leutwyler, D., Schär, C. and Fosser, G.: Pan-European climate at convection-permitting scale: a model intercomparison study. Clim Dyn 55, 35–59, https://doi.org/10.1007/s00382-018-4114-6, 2020.

Brienen, S., Haller, M., Brauch, J., Früh, B.: HoKliSim-De evaluation simulation with COSMO-CLM5-0-16 version V2022.01, 10.5676/DWD/HOKLISIM_V2022.01, 2022.

Caldas-Alvarez, A., Augenstein, M., Ayzel, G., Barfus, K., Cherian, R., Dillenardt, L., Fauer, F., Feldmann, H., Heistermann, M., Karwat, A., Kaspar, F., Kreibich, H., Lucio-Eceiza, E. E., Meredith, E. P., Mohr, S., Niermann, D., Pfahl, S., Ruff, F., Rust, H. W., Schoppa, L., Schwitalla, T., Steidl, S., Thieken, A. H., Tradowsky, J. S., Wulfmeyer, V., and Quaas, J.: Meteorological, impact and climate perspectives of the 29 June 2017 event, Nat. Hazards Earth Syst. Sci., 22, 3701–3724, https://doi.org/10.5194/nhess-22-3701-2022, 2022.

Da Silva, N.A. and Haerter, J. O.: Super-Clausius–Clapeyron scaling of extreme precipitation explained by shift from stratiform to convective rain type, Nat. Geosci. 18, 382–388, https://doi.org/10.1038/s41561-025-01686-4, 2025.

Dallan, E., Marra, F., Fosser, G., Marani, M., Formetta, G., Schär, C., and Borga, M.: How well does a convection-permitting regional climate model represent the reverse orographic effect of extreme hourly precipitation?, Hydrol. Earth Syst. Sci., 27, 1133 – 1149, https://doi.org/10.5194/hess-27-1133-2023, 2023.

Fauer, F. S., Ulrich, J., Jurado, O. E., and Rust, H. W.: Flexible and consistent quantile estimation for intensity–duration–frequency curves, Hydrol. Earth Syst. Sci., 25, 6479–6494, https://doi.org/10.5194/hess-25-6479-2021, 2021.

Flato, G., Marotzke, J., Abiodun, B., Braconnot, P., Chou, S. C., Collins, W., Cox, P., Driouech, F., Emori, S., Eyring, V., Forest, C., Gleckler, P., Guilyardi, E., Jakob, C., Kattsov, V., Reason, C. and Rummukainen, M.: Evaluation of climate models, in: Climate Change 2013: The Physical Science Basis, Cambridge University Press, 741–882, https://doi.org/10.1017/CBO9781107415324.020, 2013.

Forster, P. M., T.Andrews, P.Good, J. M.Gregory, L. S.Jackson, and M.Zelinka.: Evaluating adjusted forcing and model spread for historical and future scenarios in the CMIP5 models, J. Climate, 26, 4394–4413, https://doi.org/10.1002/jgrd.50174, 2013.

Gimeno, L., Sorí, R., Vázquez, M., Stojanovic, M., Algarra, I., Eiras-Barca, J., Gimeno-Sotelo, L., & Nieto, R.: Extreme precipitation events, WIREs Water, 9, e1611, https://doi.org/10.1002/wat2.1611, 2022.

Lenderink, G., de Vries, H., Fowler, H. J., Barbero, R., van Ulft, B., and van Meijgaard, E.: Scaling and responses of extreme hourly precipitation in three climate experiments with a convection-permitting model, Philos Trans A Math Phys Eng Sci; 379 (2195): 20190544, https://doi.org/10.1098/rsta.2019.0544, 2021.

Lenderink, G., Barbero, R., Loriaux, J. M., and Fowler, H. J.: Super-Clausius-Clapeyron scaling of extreme hourly convective precipitation and its relation to large-scale atmospheric conditions, J. Climate, 30, 6037–6052, https://doi.org/10.1175/JCLI-D-16-0808.1, 2017.

Guan, X., Nguyen, V. D., Voit, P., Merz, B., Heistermann, M., and Vorogushyn, S.: The ability of a stochastic regional weather generator to reproduce heavy-precipitation events across scales, Nat. Hazards Earth Syst. Sci., 25, 3075–3086, https://doi.org/10.5194/nhess-25-3075-2025, 2025.

Haller, M., Brienen, S., Brauch, J., and Früh, B.: Historical simulation with COSMO-CLM5-0-16 version V2022.01, DWD Climate Prediction System data set, https://doi.org/10.5676/DWD/CPS_HIST_V2022.01, 2022a.

Haller, M., Brienen, S., Brauch, J., and Früh, B.: Projection simulation with COSMO-CLM5-0-16 version V2022.01, DWD Climate Prediction System data set, https://doi.org/10.5676/DWD/CPS_SCEN_V2022.01, 2022b.

Haslinger, K., Breinl, K., Pavlin, L., Pistotnik, G., Bertola M., Olefs M., Greilinger M., Schöner W., and Blöschl G.: Increasing hourly heavy rainfall in Austria reflected in flood changes, Nature, 639, 667–672, https://doi.org/10.1038/s41586-025-08647-2, 2025.

Hosseinzadehtalaei, P., Tabari, H., and Willems, P.: Climate change impact on short-duration extreme precipitation and intensity–duration–frequency curves over Europe, J. Hydrol., 590, 125249, https://doi.org/10.1016/j.jhydrol.2020.125249, 2020.

Huang, H., Cui, H., and Ge, Q.: Assessment of potential risks induced by increasing extreme precipitation under climate change, Nat. Hazards, 108, 2059–2079, https://doi.org/10.1007/s11069-021-04768-9, 2021.

Khazai, B., Bessel, T., Möhrle, S., Dittrich, A., Schröter, K., Mühr, B., Elmer, F., Kunz-Plapp, T., Trieselmann, W., and Kunz, N.: June Flood 2013 flood in Central Europe – Focus Germany, CEDIM Report, 2013.

Kotz, M., Lange, S., Wenz, L., and Levermann, A.: Constraining the pattern and magnitude of projected extreme precipitation change in a multimodel ensemble, J. Climate, 97–111, https://doi.org/10.1175/JCLI-D-23-0492.1, 2023.

Koutsoyiannis, D., Kozonis, D., and Manetas, A.: A mathematical framework for studying rainfall intensity–duration–frequency relationships, J. Hydrol., 206, 118–135, https://doi.org/10.1016/S0022-1694(98)00097-3, 1998.

Kuma, P., Bender, F. A.-M., and Jönsson, A. R.: Climate model code genealogy and its relation to climate feedbacks and sensitivity. Journal of Advances in Modeling Earth Systems, 15, e2022MS003588, https://doi.org/10.1029/2022MS003588, 2023.

Lengfeld, K., Walawender, E., Winterrath, T., and Becker, A.: A catalogue of radar-based heavy rainfall events in Germany derived from 20 years of data, Meteorol. Z., 30, 469–487, https://doi.org/10.1127/metz/2021/1088, 2021.

Lengfeld, K., Voit, P., Kaspar, F., and Heistermann, M.: Brief communication: On the extremeness of the July 2021 precipitation event in western Germany, Nat. Hazards Earth Syst. Sci., 23, 1227–1232, https://doi.org/10.5194/nhess-23-1227-2023, 2023.

Lennartz, M., Poschlod, B., and Merz, B.: Benefits of the simplified MEV for analyzing hourly precipitation extremes in a changing climate, EGUsphere [preprint], https://doi.org/10.5194/egusphere-2025-6419, 2026.

Lucas-Picher, P., Argüeso, D., Brisson, E., Tramblay, Y., Berg, P., Lemonsu, A., Kotlarski, S., and Caillaud, C.: Convection-permitting modeling with regional climate models: Latest developments and next steps. Wiley Interdisciplinary Reviews: Climate Change, 12(6), e731. https://doi.org/10.1002/wcc.731, 2021.

Madsen, H., Lawrence, D., Lang, M., Martinkova, M., and Kjeldsen, T. R.: Review of trend analysis and climate change projections of extreme precipitation and floods in Europe, J. Hydrol., 519, 3634–3650, https://doi.org/10.1016/j.jhydrol.2014.11.003, 2014.

Martel, J.-L., Brissette, F. P., Lucas-Picher, P., Troin, M., and Arsenault, R.: Climate change and rainfall intensity–duration–frequency curves: Overview of science and guidelines for adaptation, J. Hydrol. Eng., 26, https://doi.org/10.1061/(ASCE)HE.1943-5584.0002122, 2021.

Matte, D., Christensen, J. H., and Ozturk, T.: Spatial extent of precipitation events: when big is getting bigger, Clim. Dyn., 58, 1861–1875, https://doi.org/10.1007/s00382-021-05998-0, 2022.

Munz, L., Mosimann, M., Kauzlaric, M., Martius, O., and Zischg, A, P.: Storylines of extreme precipitation events and flood impacts in alpine and pre-alpine environments under various global warming levels, Sci. Total Environ., 957, 177791, https://doi.org/10.1016/j.scitotenv.2024.177791, 2024.

Müller, M. and Kaspar, F.: Event-adjusted evaluation of weather and climate extremes, Nat. Hazards Earth Syst. Sci., 14, 473–483, https://doi.org/10.5194/nhess-14-473-2014, 2014.

Nissen, K. M. and Ulbrich, U.: Increasing frequencies and changing characteristics of heavy precipitation events threatening infrastructure in Europe under climate change, Nat. Hazards Earth Syst. Sci., 17, 1177–1190, https://doi.org/10.5194/nhess-17-1177-2017, 2017.

Piper, D., Kunz, M., Ehmele, F., Mohr, S., Mühr, B., Kron, A., and Daniell, J.: Exceptional sequence of severe thunderstorms and related flash floods in May and June 2016 in Germany – Part 1: Meteorological background, Nat. Hazards Earth Syst. Sci., 16, 2835–2850, https://doi.org/10.5194/nhess-16-2835-2016, 2016.

Poschlod, B., Ludwig, R., and Sillmann, J.: Ten-year return levels of sub-daily extreme precipitation over Europe, Earth Syst. Sci. Data, 13, 983–1003, https://doi.org/10.5194/essd-13-983-2021, 2021.

Poschlod, B. and Ludwig, R.: Internal variability and temperature scaling of future sub-daily rainfall return levels over Europe, Environ. Res. Lett., 16, 064097, https://doi.org/10.1088/1748-9326/ac0849, 2021.

Poschlod, B. and Koh, J.: Convection-permitting climate models can support observations to generate rainfall return levels. Water Resources Research, 60, e2023WR035159. https://doi.org/10.1029/2023WR035159, 2024.

Prein, A., Rasmussen, R., Ikeda, K., Liu, C., Clark, M., Holland, G.: The future intensification of hourly precipitation extremes, Nat. Clim. Change, 7, 48–52, https://doi.org/10.1038/nclimate3168, 2017.

Pöschmann, J. M., Kim, D., Kronenberg, R., and Bernhofer, C.: An analysis of temporal scaling behaviour of extreme rainfall in Germany, Nat. Hazards Earth Syst. Sci., 21, 1195–1207, https://doi.org/10.5194/nhess-21-1195-2021, 2021.

Purr, C., Brisson, E., and Ahrens, B.: Convective rain cell characteristics and scaling in climate projections for Germany, Int. J. Climatol., 41, 3174–3185, https://doi.org/10.1002/joc.7012, 2021.

Purr, C., Brisson, E., Schlünzen, K. H., and Ahrens, B.: Convective rain cell properties and the resulting precipitation scaling in a warm-temperate climate, Q. J. R. Meteorol. Soc., 148, 1611–2062, https://doi.org/10.1002/qj.4277, 2022.

Riahi, K., Rao, S., Krey, V., Cho, C., Chirkov, V., Fischer, G., Kindermann, G., Nakicenovic, N. and Rafaj, P.: RCP8.5 – A scenario of comparatively high greenhouse gas emissions, Clim. Change, 109, 33–57, https://doi.org/10.1007/s10584-011-0149-y, 2011.

Rischmuller, A. L., Poschlod, B., and Sillmann, J.: Bayesian hierarchical modelling of intensity-duration-frequency curves using a climate model large ensemble, Adv. Stat. Clim. Meteorol. Oceanogr., 12, 1–19, https://doi.org/10.5194/ascmo-12-1-2026, 2026.

Rybka, H., Haller, M., Brienen, S., Brauch, J., Früh, B., Junghänel, T., Lengfeld, K., Walter, A., and Winterrath, T.: Convection-permitting climate simulations with COSMO-CLM for Germany: analysis of present and future daily and sub-daily extreme precipitation, Meteorol. Z., 32, 91–111, https://doi.org/10.1127/metz/2022/1147, 2023.

Sakamoto, T. T., Komuro, Y., Nishimura, T., Ishii, M., Tatebe, H., Shiogama, H., Hasegawa, A., Toyoda, T., Mori, M., Suzuki, T., Imada, Y., Nozawa, T., Takata, K., Mochizuki, T., Ogochi, K., Emori, S., Hasumi, H., and Kimoto, M.: MIROC4h – A new high-resolution atmosphere–ocean coupled general circulation model. Part II: climate sensitivity and feedback analysis, J. Meteorol. Soc. Jpn., 90A, 325–364, https://doi.org/10.2151/jmsj.2012-301, 2012.

Schroeer, K. and Kirchengast, G.: Sensitivity of extreme precipitation to temperature: the variability of scaling factors from a regional to local perspective, Clim Dyn 50, 3981–3994, https://doi.org/10.1007/s00382-017-3857-9, 2018.

Sørland, S. L., Brogli, R., Pothapakula, P. K., Russo, E., Van de Walle, J., Ahrens, B., Anders, I., Bucchignani, E., Davin, E. L., Demory, M.-E., Dosio, A., Feldmann, H., Früh, B., Geyer, B., Keuler, K., Lee, D., Li, D., van Lipzig, N. P. M., Min, S.-K., Panitz, H.-J., Rockel, B., Schär, C., Steger, C., and Thiery, W.: COSMO-CLM regional climate simulations in the EURO-CORDEX framework: a review, Geosci. Model Dev., 14, 5125–5154, https://doi.org/10.5194/gmd-14-5125-2021, 2021.

Sperber, K. R., Annamalai, H., Kang, I. S., Kitoh, A., Moise, A., Turner, A., Wang, B. and Zhou, T.: The Asian summer monsoon: an intercomparison of CMIP5 vs CMIP3 simulations of the late 20th century, Clim. Dyn., 41, 2711–2744, https://doi.org/10.1007/s00382-012-1607-6, 2013.

Thieken, A. H., Kienzler, S., Kreibich, H., Kuhlicke, C., Kunz, M., Mühr, B., Müller, M., Otto, A., Petrow, T., Pisi, S., and Schröter, K.: Review of the flood risk management system in Germany after the major flood in 2013, Ecol. Soc., 21, 51, https://doi.org/10.5751/ES-08547-210251, 2016.

Thieken, A. H., Samprogna Mohor, G., Kreibich, H., and Müller, M.: Compound inland flood events: different pathways, different impacts and different coping options, Nat. Hazards Earth Syst. Sci., 22, 165–185, https://doi.org/10.5194/nhess-22-165-2022, 2022.

Ulrich, J., Jurado, O. E., Peter, M., Scheibel, M., and Rust, H. W.: Estimating IDF curves consistently over durations with spatial covariates, Water, 12, 3119, https://doi.org/10.3390/w12113119, 2020.

Vautard, R., Kadygrov, N., Iles, C., Boberg, F., Buonomo, E., Bülow, K., Coppola, E., Corre, L., van Meijgaard, E., Nogherotto, R., Sandstad, M., Schwingshackl, C., Somot, S., Aalbers, E., Christensen, O. B., Ciarlo, J. M., Demory, M.-E., Giorgi, F., Jacob, D., Jones, R. G., Keuler, K., Kjellström, E., Lenderink, G., Levavasseur, G., Nikulin, G., Sillmann, J., Solidoro, C., Sørland, S. L., Steger, C., Teichmann, C., Warrach-Sagi, K., and Wulfmeyer, V.: Evaluation of the large EURO-

CORDEX regional climate model ensemble, J. Geophys. Res. Atmos., 126, e2019JD032344, https://doi.org/10.1029/2019JD032344, 2021.

Voit, P. and Heistermann, M.: A new index to quantify the extremeness of precipitation across scales, Nat. Hazards Earth Syst. Sci., 22, 2791–2805, https://doi.org/10.5194/nhess-22-2791-2022, 2022.

Watanabe, M., Suzuki, T., O'ishi, R., Komuro, Y., Watanabe, S., Emori, S., Takemura, T., Chikira, M., Ogura, T., Sekiguchi, M., Takata, K., Yamazaki, D., Yokohata, T., Nozawa, T., Hasumi, H., Tatebe, H., and Kimoto, M.: Improved climate simulation by MIROC5: mean states, variability, and climate sensitivity, J. Climate, 23, 6312–6335, https://doi.org/10.1175/2010JCLI3679.1, 2011.

Westra, S., Fowler, H. J., Evans, J. P., Alexander, L. V., Berg, P., Johnson, F., Kendon, E. J., Lenderink, G., and Roberts, N. M.: Future changes to the intensity and frequency of short-duration extreme rainfall, Rev. Geophys., 52, 522–555, https://doi.org/10.1002/2014RG000464, 2014.

Yang, J. xWEI calculation for the top 200 precipitation events over Germany based on convection-permitting climate simulations. Zenodo. https://doi.org/10.5281/zenodo.19877857, 2026.

Zeder, J. and Fischer, E. M.: Observed extreme precipitation trends and scaling in Central Europe, Weather Clim. Extremes, 29, 100266, https://doi.org/10.1016/j.wace.2020.100266, 2020.